LWT - Food Science and Technology 176 (2023) 114552

Contents lists available at ScienceDirect

LWT

journal homepage: www.elsevier.com/locate/lwt

Mathematical modelling of drying kinetics of avocado peels and its influence on flavan-3-ols content and antioxidant activity

María del Carmen Razola-Díaz [a], Eduardo Jesús Guerra-Hernández [a], Ana María Gómez-Caravaca [c,*], Belén García-Villanova [a], Vito Verardo [a,b,**]

[a] Department of Nutrition and Food Science, University of Granada, Campus of Cartuja, 18011, Granada, Spain
[b] Institute of Nutrition and Food Technology 'José Mataix', Biomedical Research Centre, University of Granada, Avda del Conocimiento sn, 18100, Granada, Spain
[c] Department of Analytical Chemistry, Faculty of Sciences, University of Granada, Avda Fuentenueva s/n, 18071, Granada, Spain

ARTICLE INFO

Keywords:
HPLC-FLD
Avocado by-product
Avocado wastes
Air-drying
Polyphenols

ABSTRACT

Avocado peel is one of the main by-products of avocado processing and is considered a promising source of phenolic compounds with various bioactivities. The drying step is essential for its storage at the industrial level, and it is the first step in the strategy of transforming by-products into functional ingredients. Therefore, this research evaluates the effect of the convective air-drying of avocado peels at three different temperatures (40, 60 and 80 °C) and airflows (0, 0.8 and 1.6 m/s) on the flavan-3-ols content and antioxidant activity. Moreover, the mathematical modelling of its drying kinetic was developed. A decrease in the flavan-3-ol and antioxidant content was found with increasing temperatures. However, a high impact of the airflow reducing the drying time and limiting the decrease in interesting compounds was found. Among the tested mathematical models, the Page model reported the highest values of R^2 (from 0.9907 to 0.9973) and the lowest errors for most of the temperatures and airflows tested. However, at 80 °C with airflow, the Lewis model seemed to fit better (R^2 = 0.9982). Finally, the drying conditions that showed the lowest decrease in procyanidin and antioxidants were 40 °C and an airflow of 1.6 m/s for 105 min.

1. Introduction

Worldwide avocado (*Persea americana*) production has been growing, reaching a volume of 8.02 million tons in 2020. The largest producing countries of avocado are those with subtropical climate conditions, such as México, Dominican Republic and Perú. In 2019 the avocado industry had a worldwide value of 12.82 billion dollars, which is expected to increase over the next five years. In this context, avocado production in Spain is also constantly growing. In the last three years, it has increased from 89.7 thousand tons in 2018 to 95.5 thousand tons in 2019 and to 107.9 thousand tons in 2020. Moreover, in 2020 Spain was the third and fourth worldwide country in exporting and importing avocados, with values of 442.89 and 389.3 million dollars, respectively (*Statista - The Statistics Portal for Market Data, Market Research and Market Studies*, n.d.). However, all these movements and avocado production are increasing waste generation, which also has economic and environmental costs.

Avocado by-products are industrial waste generated during the processing of avocado fruit, principally composed of peels and seeds (García-Vargas et al., 2020). These by-products are a potential source of bioactive compounds with various bioactivities, such as antimicrobial, anti-inflammatory, anticancer, antidiabetic and antihypertensive (Araújo et al., 2018). Special attention has been paid to agro-industrial waste because of its potential use in developing high-value-added products such as nutraceuticals or cosmeceuticals while reducing its environmental impact (Jimenez et al., 2021). In this context, finding the best procedure to take advantage of these by-products should be an important research focus. Especially avocado peel is a well-known source of polyphenols such as phenolic acids and flavonoids such as (epi)catechin and its derivatives procyanidins at different degrees of polymerization. However, the concentration and stability of these compounds are affected by several factors, such as the avocado variety, light and oxygen exposure, pH, storage temperature and extraction solvents and procedure.

* Corresponding author.
** Corresponding author. Department of Nutrition and Food Science, University of Granada, Campus of Cartuja, 18011, Granada, Spain.
E-mail addresses: carmenrazola@ugr.es (M.C. Razola-Díaz), ejguerra@ugr.es (E.J. Guerra-Hernández), anagomez@ugr.es (A.M. Gómez-Caravaca), belenvb@ugr.es (B. García-Villanova), vitoverardo@ugr.es (V. Verardo).

https://doi.org/10.1016/j.lwt.2023.114552
Received 2 July 2022; Received in revised form 30 January 2023; Accepted 1 February 2023
Available online 2 February 2023

Drying is one of the most common and extended processes used to preserve quality and stability and to extend the shelf-life of fruits, vegetables, and their by-products. It reduces the moisture content and water activity avoiding spoilage during management and storage (Colombo & Papetti, 2019). Among all the different techniques used in this scope, convective drying has been demonstrated to be the most scalable and cheapest at the industrial scale (McMinn & Magee, 1999). Finding the best conditions to dry avocado peels is important, and some aspects should be considered. Temperature is important because the bioactive and antioxidant compounds are thermolabile, and high temperature could lead to their destruction. Moreover, in economic and industrial terms, the drying process should be short and low energy consuming. Furthermore, drying involves a simultaneous transference of heat and mass, turning it into a complex phenomenon. Therefore, using mathematical models to simulate its kinetic and explain the mechanism of the water transference during this operation is a useful tool to control the process (Castro et al., 2018).

Some authors have evaluated the effect of drying on some parameters of the avocado peel (Babiker et al., 2021; Figueroa et al., 2018); however, they did not discuss its drying kinetic. Avhad and Marchetti (2016) described the drying behaviour of 'Hass' avocado seeds using four mathematical models. Saavedra et al. (2017) analysed the avocado by-product drying kinetics using the Lewis model, but no other more complex models were considered. Moreover, they optimised the convective drying process in avocado peel by focusing on the total phenolic content measured using Folin-Ciocalteu reagent. Alkaltham et al. (2021) evaluated the effect of different drying techniques on the polyphenol content in different parts of avocado. They reported catechin concentrations of 99.11, 180.37 and 62.52 mg/100g in ripe pulp, peel and seeds, respectively, of avocado oven-dried at 60 °C measured using high-performance liquid chromatography (HPLC) with photodiode array detector (PDA). According to these authors, the avocado peel is the richest avocado part in catechins and, by extension, in flavan-3-ols. However, its drying kinetics have not been completely studied to date. Moreover, according to Vidal-Casanella et al. (2022), the HPLC with a fluorometric detector (FLD) showed better selectivity and sensitivity for measuring flavan-3-ols compositions of fruit samples being simpler, cheaper, and more robust alternative than other sophisticated methods, such as those based on HPLC-mass spectrometry (MS). To our knowledge, the influence of air convective drying on the procyanidin content of the avocado by-products has never been reported before.

Considering the above, the aim of the present research is to evaluate the effect of convective air-drying of avocado peels targeting their procyanidin content and antioxidant activity. It is the first step in transforming these by-products into functional ingredients or nutraceuticals. Moreover, the mathematical modelling of its drying kinetic was developed using fourteen different models to investigate the avocado peel behaviour and to find the model that fits the best.

2. Materials and methods

2.1. Chemicals and samples

Catechin, Trolox, DPPH (1,1-diphenyl-2-(2,4,6-trinitrophenyl) hydrazine), ABTS (2,2′-azino-bis(3-ethylbenzothiazoline-6-sulfonic acid)) and FRAP (ferric reducing antioxidant power) reagents with purity ≥98% in all cases were acquired from Sigma-Aldrich (St. Louis, MO, USA). Water was purified using a Milli-Q system (Millipore, Bedford, MA, USA). HPLC grade water reagent and other reagents and solvents were purchased from Merck KGaA (Darmstadt, Germany).

The avocado by-product from the variety "Hass" was obtained from a company located in Motril, on the subtropical coast of Granada province, Spain, in October 2020. The by-product was obtained directly after the industrial processing for obtaining guacamole. It was maintained at 5 °C and then the samples were dried, milled and sieved to 100 μm and remained at −18 °C till analysis.

Table 1
Mathematical drying models fitted to the drying curves of avocado peels.

Model	Equation	References
Lewis	$MR = e^{(-kt)}$ (5)	(Berbert et al., 2019; Lewis, 1921; Ozarslan & Bas, 2020; Penteado-Rosa et al., 2015)
Henderson and Pabis	$MR = ae^{(-kt)}$ (6)	(Corrêa et al., 2019; Dikmen et al., 2019; Henderson, 1961; Vega-Gálvez et al., 2010; Yang et al., 2007)
Page	$MR = e^{(-kt^N)}$ (7)	(Falade & Solademi, 2010; Ghodake et al., 2006; Górnicki et al., 2020; Karathanos & Belessiotis, 1999; Zhao et al., 2022)
Logarithmic	$MR = a\,e^{-kt} + c$ (8)	(Togrul & Pehlivan, 2002; Xu et al., 2022; Yaldýz & Ertekýn, 2001; Zhao et al., 2022)
Avhad and Marchetti	$MR = a\,e^{(-kt^n)}$ (9)	Avhad and Marchetti (2016)
Wang and Singh	$MR = 1 + at + bt^2$ (10)	(de Brito Araújo et al., 2021; Wang & Singh, 1978)
Parabolic	$MR = a + bt + ct^2$ (11)	Kohli et al. (2022)
Polynomial	$MR = a + bt + ct^2 + dt^3$ (12)	Haghi and Ghanadzadeh (2005)
Thompson	$t = a \ln MR + b (\ln MR)^2$ (13)	(Gaikwad et al., 2022; Togrul & Pehlivan, 2002)
Geometric	$MR = a\,t^{-n}$ (14)	Shen et al. (2020)
Verma	$MR = a\,e^{(-k_1 t)} + (1-a)e^{(-k_2 t)}$ (15)	(An et al., 2022; Gaikwad et al., 2022)
Two-factor	$MR = a\,e^{(-k_1 t)} + b\,e^{(-k_2 t)}$ (16)	(Gaikwad et al., 2022; Sahoo et al., 2022)
Midilli	$MR = a\,e^{(-kt^n)} + b\,t$ (17)	(Ferreira et al., 2021; Gaikwad et al., 2022)
Weibull	$MR = a - b\,e^{(-kt^n)}$ (18)	(Gaikwad et al., 2022; Nguyen et al., 2022; Vega-Gálvez et al., 2010)

2.2. Drying process and kinetic

Samples of avocado peels were dried by convective drying using an oven (Memmert, Schwabach, Germany). The weight loss was measured manually with a precision manual balance (Sartorius, Gotinga, Germany) in less than 15 s until the moisture content was below 10% (Deng et al., 2020).

Similarly to other authors (Ferreira et al., 2021; Llavata et al., 2022; Loh & Lim, 2018; Saavedra et al., 2017; Vega-Gálvez et al., 2009; Yamassaki et al., 2017), the temperatures tested were 40, 60 and 80 °C. In addition, three different airflows were tested according to the oven possibilities: 0, 0.8 and 1.6 m/s.

At each time point, the moisture content was expressed as moisture ratio (MR) according to the weight loss and solid content remaining, a dimensionless term calculated from equation (1):

$$MR = \frac{M_t - M_e}{M_0 - M_e} \quad (1)$$

where M_0, M_t and M_e are the moisture content (g/g dry weight (d.w.)) at the initial time, time t, and equilibrium, respectively.

The drying rate (DR) was calculated to express the moisture loss per unit of time, which can be calculated according to equation (2):

$$DR = \frac{M_{t1} - M_{t2}}{t_2 - t_1} \quad (2)$$

where M_{t1} and M_{t2} are the moisture content (g/g d.w.) at the time points t_1 and t_2, respectively.

The effective moisture diffusivity (D_{eff}) was calculated according to Fick's second law when assuming that the sample shrinkage is negligible. Therefore, the initial moisture distribution is uniform, and the moisture diffusivity is constant, as shown in equation (3):

$$MR = \left(\frac{8}{\pi^2}\right)e^{\left(-\frac{\pi^2 D_{eff}}{4L^2}t\right)} \quad (3)$$

where MR, D_{eff}, L and t are the moisture ratio, effective moisture diffusivity, the half-thickness of the sample (m) and the time (min), respectively.

Additionally, the Arrhenius equation was used to calculate the activation energy (Ea) described in equation (4):

$$D_{eff} = Ae^{(-Ea/RT)} \quad (4)$$

where D_{eff}, A, Ea, R and T are the effective moisture diffusivity, the pre-exponential factor of the Arrhenius equation, the activation energy (KJ/mol), the universal gas constant (8.314 J/mol K) and the temperature (K), respectively.

Finding the best-fitting model for avocado by-product drying behaviour is extremely important to predict its drying kinetics accurately. The drying mathematical modelling has been studied recently in other fruits and vegetables such as asparagus root (Kohli et al., 2022), dragon fruit (Joseph Bassey et al., 2022), edamame (An et al., 2022), pomelo albedo (Nguyen & Le, 2022), uvaia fruit (Gomes et al., 2022), yam (Sahoo et al., 2022), *Ascophyllum Nodosum* (Zhu et al., 2021) or black gram papad (Gaikwad et al., 2022).

Therefore, the experimental drying data was fitted with fourteen semi-theoretical drying mathematical models for the three different temperatures and the three different airflows, and the mathematical equations (5-18) are shown in Table 1, where MR is the moisture ratio, a, b, c, n, N and k are model constants and t is the time.

2.3. Statistical parameters

Various statistical parameters were used to select the best mathematical model that predicts the drying kinetics of avocado peels, such as the coefficient of determination (R^2), defined by Taylor (1997). Furthermore, other statistical parameters previously used by other authors (Avhad & Marchetti, 2016; Gaikwad et al., 2022; Kohli et al., 2022) were also used for this purpose, such as chi-square error (X^2), the standard error of estimation (SEE), root mean square error (RMSE), the mean absolute error (MAE) and the relative mean error (P_0). Overall, these terms indicate how close the experimental data and the prediction are. They were calculated for all three temperatures at the three different airflows for all the proposed mathematical models. A model is considered to have a high-quality fit when the R^2 value is close to 1 and the X^2, SEE, RMSE and MAE values are close to 0. Moreover, the model is acceptable or fits well when $P_0 < 0.5$ (Castro et al., 2018). The mentioned statistical parameters were calculated according to equations 19–24, where the experimental and predicted dimensionless moisture ratios are expressed as $MR_{exp,i}$ and $MR_{pred,i}$, respectively. N represents the number of observations, and i denotes the number of constants in the model.

$$R^2 = \frac{\sum_{i=1}^{N}\left(MR_{exp,i} - \overline{MR}_{pred,i}\right) * \left(MR_{pred,i} - \overline{MR}_{exp,i}\right)}{\sqrt{\sum_{i=1}^{N}\left(MR_{exp,i} - \overline{MR}_{pred,i}\right)^2 * \sum_{i=1}^{N}\left(MR_{exp,i} - \overline{MR}_{pred,i}\right)^2}} \quad (19)$$

$$X^2 = \frac{\sum_{i=1}^{N}\left(MR_{exp,i} - MR_{pred,i}\right)^2}{N - z} \quad (20)$$

$$SEE = \sqrt{\frac{\sum_{i=1}^{N}\left(MR_{exp,i} - MR_{pred,i}\right)^2}{N - n_i}} \quad (21)$$

$$RMSE = \sqrt{\frac{\left(\sum_{i=1}^{N} MR_{exp,i} - \sum_{i=1}^{N} MR_{pred,i}\right)^2}{N}} \quad (22)$$

$$MAE = \frac{1}{N}\sum_{i=1}^{N}\left(MR_{pred,i} - MR_{exp,i}\right) \quad (23)$$

$$P_0 = \frac{1}{N}\sum_{i=1}^{N}\left|\frac{\left(MR_{exp,i} - MR_{pred,i}\right)}{MR_{exp,i}}\right| \quad (24)$$

2.4. Ultrasound extraction

Briefly, 2 g of avocado by-product powder was added to 15 mL of ethanol/water solution (80:20 v/v). The mixture was placed in an ultrasonic bath (Bandelin, Sonorex, RK52, Berlin, Germany) which worked at a frequency of 35 kHz and 60 W for 15 min; then, it was centrifuged for 10 min at 8603×*g*. The supernatant was collected, and the extraction was repeated twice more. Finally, the supernatants were evaporated and reconstituted in 1 mL of methanol/water (50:50, v/v). The final extracts were filtered with regenerated cellulose filters 0.2 μm (Millipore, Bedford, MA, USA) and stored at −18 °C until the analyses.

2.5. Antioxidant assays

The antioxidant activity was evaluated in all the samples by three different methods in duplicate. The DPPH assay was performed according to a method proposed by several authors (Brand-Williams et al., 1995; Parejo et al., 2000). Briefly, 100 μL of each extract was added to 2.9 mL of $DPPH^{\bullet}$ solution, and after rapid stirring, the bleaching power of the extract was observed in a time interval from 0 to 30 min at 517 nm. The ABTS method was performed according to the protocol of Re et al. (1999). The monocation $ABTS^{\bullet+}$ is generated by oxidation of the ABTS with potassium persulfate in the dark at room temperature for 12–24 h. For each extract, 1 mL of this $ABTS^{\bullet+}$ solution was added to 0.01 mL. Then, the decrease in absorbance was measured for 30 min at 734 nm. The FRAP assay was conducted following the procedure developed by Pulido et al. (2000). It is based on the reduction of Fe^{3+} to Fe^{2+} by the antioxidant substances. Briefly, 30 μl of each extract were added to 90 μL of distilled water and 900 μL of the FRAP reagent. The resulting solution was kept for 30 min at 37 °C; then, absorbance was measured in the spectrophotometer at 595 nm. Standard curves of Trolox equivalents (TE) (1, 5, 10, 20, 50, 80, 100, 150, 200 μg/g) were generated for each assay. Results are expressed as mg TE/g d.w.

2.6. HPLC-FLD analysis

The methodology used to determine flavan-3-ols was previously reported by López-Cobo et al. (2016). An Agilent 1200 Series (Agilent Technologies, Palo Alto, CA, USA) equipped with a quaternary pump delivery system, a degasser, an autosampler and a FLD was used for the analyses. A Develosil Diol 100 Å column 5 mm, 250 × 4.6 mm ID (Phenomenex, Torrance, CA, USA) was used. Mobile phase A and B consisted of an acidic acetonitrile ((A), CH3CN:CH3COOH, 98:2; v/v) and acidic aqueous methanol ((B), CH3OH:H2O:CH3COOH, 95:3:2; v/v/v). The gradient elution was: 3% B for 50 min, 38% B for 3 min, 100% B for 13 min and 100% B for 10 min. Then the initial conditions were set, 0% B for 10 min. Fluorescence detection was performed with an excitation wavelength of 230 nm and an emission wavelength of 321 nm. The injection volume was 10 μL. All the analyses were conducted at 35 °C. The identification of flavan-3-ols was performed according to the previously described (López-Cobo et al., 2016), as they are eluted according to their degree of polymerization, firstly eluting the monomers and then the different oligomers (Robbins et al., 2009). A standard curve of catechin at 6 concentrations from 10 to 650 μg/g was generated to quantify flavan-3-ols. In addition, the correction factors suggested by Robbins et al. (2009) were used. The results are expressed as mg catechin equivalents (CE)/g d.w.

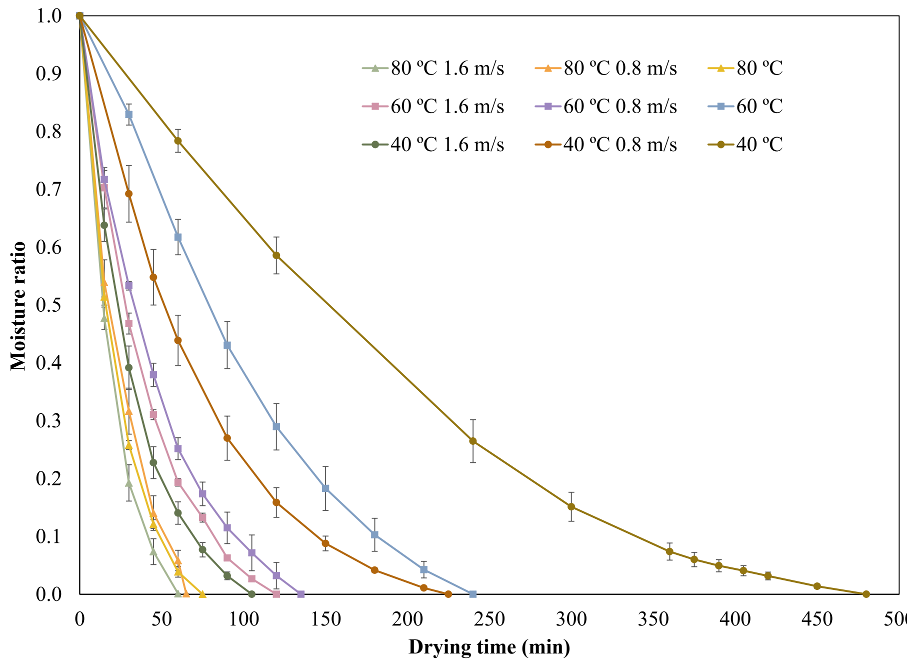

Fig. 1. Drying kinetics curves of avocado peel under different temperatures and airflows.

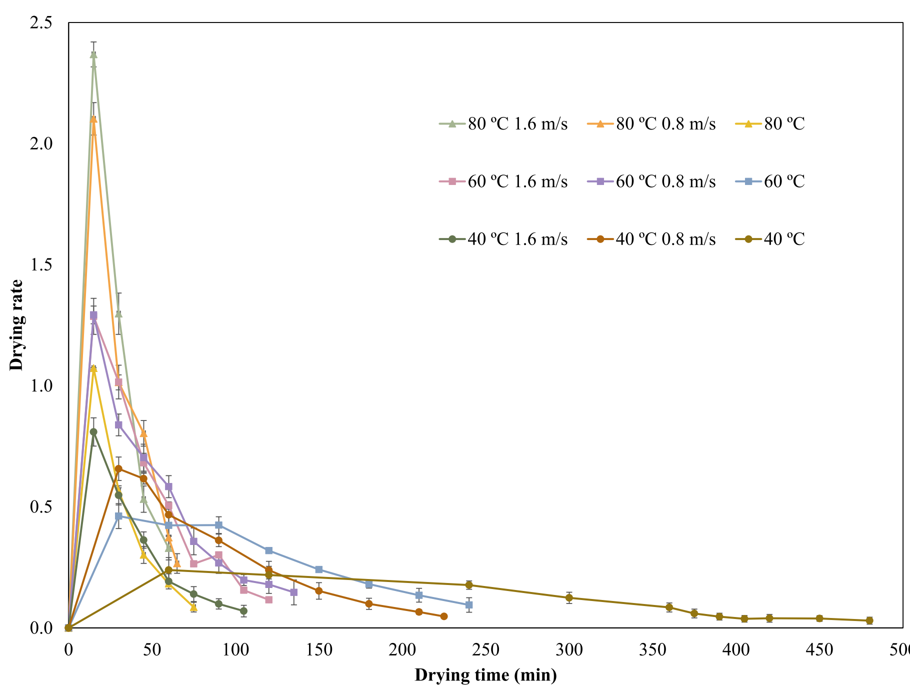

Fig. 2. Drying rate curves of avocado peel under different temperatures and airflows.

3. Results and discussion

3.1. Drying kinetics and modelling

Fig. 1 shows the drying curve of avocado peel, where the changes in the moisture ratio of the avocado peel over the time at different temperatures (40, 60 and 80 °C) and airflows (0, 0.8 and 1.6 m/s) are represented. Without airflow, the drying time required to achieve the final moisture content of the avocado by-product was 75, 240 and 480 min at 80, 60 and 40 °C, respectively. Özbek et al. (2022) reported a drying time of 180 min when using hot air-drying at 50 °C in avocado pulp, demonstrating the differences between various parts of the avocado. The temperature has a high influence on the drying of the avocado peel because less time was needed to reach the lowest moisture ratio when a higher temperature was used. Similarly, the air has demonstrated its effect on drying. In this case, the decrease in the drying time with the airflow was more remarkable at lower temperatures. At 40 °C, the drying time decreased 53% when using an airflow of 0.8 m/s, and the drying time decreased 78% when the airflow was 1.6 m/s. As a combination of temperature and airflow, drying at 80 °C with an airflow of 1.6 m/s was the quickest, requiring only 60 min.

However, other parameters should be measured to evaluate and

Table 2
Results obtained for the statistical analysis for all the mathematical models at three different temperatures and airflows for avocado peels.

Model	T (°C)	Air flow 1.6 m/s						Air flow 0.8 m/s						no air flow					
		R^2	X^2	SEE	RMSE	MAE	P_0	R^2	X^2	SEE	RMSE	MAE	P_0	R^2	X^2	SEE	RMSE	MAE	P_0
Lewis	40	0.9947	7.61E-04	0.0276	0.0385	0.0222	0.1032	0.9779	0.0040	0.0635	0.1331	0.0479	0.2477	0.9801	0.0066	0.0810	0.1417	0.0488	0.2531
	60	0.9880	0.0017	0.0416	0.0724	0.0333	0.1525	0.9913	0.0012	0.0353	0.0591	0.0282	0.1223	0.9723	0.0070	0.0840	0.1414	0.0644	0.1950
	80	0.9982	7.05E-04	0.0266	0.0088	0.0190	0.0430	0.9951	0.0012	0.0339	0.0115	0.0257	0.0741	0.9937	7.21E-04	0.0268	0.0275	0.0221	0.1052
Henderson and Pabis	40	0.9882	0.0023	0.0481	0.0388	0.0289	0.0928	0.9895	0.0033	0.0573	0.0435	0.0312	0.2398	0.9499	0.0844	0.2905	0.3454	0.1221	0.2734
	60	0.9749	0.0057	0.0756	0.0574	0.0443	0.1349	0.9809	0.0036	0.0599	0.0494	0.0386	0.1160	0.9558	0.0142	0.1192	0.0716	0.0722	0.1702
	80	0.9967	0.0012	0.0348	0.0256	0.0276	0.0438	0.9894	0.0023	0.0484	0.0422	0.0354	0.0723	0.9863	0.0027	0.0515	0.0382	0.0339	0.1000
Page	40	0.9971	9.76E-05	0.0099	0.0043	0.0076	0.0542	0.9937	1.27E-04	0.0113	0.0042	0.0097	0.1224	0.9907	3.49E-04	0.0187	0.0122	0.0132	0.1316
	60	0.9940	1.72E-04	0.0131	3.56E-04	0.0104	0.0843	0.9931	2.58E-04	0.0161	2.46E-04	0.0131	0.0739	0.9973	1.93E-04	0.0139	0.0027	0.0103	0.0582
	80	0.9325	9.35E-04	0.0306	0.0147	0.0245	0.1659	0.9899	6.79E-04	0.0261	0.0166	0.0183	0.0482	0.9940	1.45E-04	0.0121	0.0047	0.0105	0.0628
Logarithmic	40	0.9882	0.0497	0.2230	0.6064	0.2144	1.9407	0.9623	0.0844	0.2905	0.8983	0.2841	4.6860	0.9493	0.1134	0.3368	1.1336	0.3272	5.7422
	60	0.9749	0.0594	0.2438	0.7128	0.2376	2.2767	0.9809	0.0526	0.2293	0.7022	0.2221	1.8379	0.9558	0.0716	0.2675	0.7640	0.2547	1.5872
	80	0.9967	0.0165	0.1285	0.2051	0.0980	0.3598	0.9894	0.0461	0.2147	0.4925	0.2011	1.1770	0.9863	0.0487	0.2207	0.5168	0.2110	1.7013
Avhad and Marchetti	40	0.9839	0.1113	0.3336	0.3597	0.1435	0.2252	0.9900	0.0169	0.1301	0.1676	0.0695	0.1999	0.9535	0.1294	0.3597	0.4134	0.1447	0.3049
	60	0.9754	0.0830	0.2882	0.3230	0.1291	0.2295	0.9718	0.0444	0.2107	0.2414	0.0975	0.1857	0.9735	0.0435	0.2086	0.2441	0.1070	0.1878
	80	0.9972	0.0199	0.1411	0.2588	0.1157	0.4929	0.9720	0.0984	0.3137	0.3405	0.1576	0.2041	0.9830	0.2260	0.4754	0.4955	0.2187	0.2960
Wang and Singh	40	0.9894	0.0238	0.1543	0.2850	0.1184	1.4497	0.9942	0.0059	0.0769	0.1795	0.0568	1.3834	0.9998	3.04E-05	0.0055	0.0029	0.0047	0.0675
	60	0.9932	8.92E-04	0.0299	0.0095	0.0256	0.2032	0.9931	0.0010	0.0318	0.0460	0.0256	0.1082	0.9983	0.0094	0.0971	0.2171	0.0724	0.5945
	80	0.9943	0.0091	0.0955	0.1547	0.0692	0.2137	0.9927	0.0099	0.0994	0.1618	0.0827	0.6273	0.9896	0.0215	0.1468	0.2316	0.1135	1.1474
Parabolic	40	0.9898	0.0100	0.1002	0.1945	0.0814	0.9668	0.9946	0.0165	0.1284	0.2854	0.0969	2.5037	0.9946	2.6585	1.6305	4.0719	1.2909	31.8451
	60	0.9935	0.0016	0.0396	0.0658	0.0348	0.4234	0.9936	0.0011	0.0337	0.0520	0.0293	0.2932	0.9984	0.0153	0.1237	0.2654	0.0929	0.7676
	80	0.9944	0.0060	0.0772	0.1150	0.0624	0.3674	0.9928	0.0043	0.0653	0.1074	0.0589	0.4286	0.9898	0.0097	0.0982	0.1607	0.0815	0.7940
Polynomial	40	0.9998	0.0094	0.0971	0.1859	0.0661	0.7774	0.9998	0.0056	0.0746	0.1731	0.0554	1.5177	0.9998	0.0019	0.0432	0.1202	0.0361	0.8143
	60	0.9997	0.0029	0.0538	0.1154	0.0389	0.5402	0.9996	0.1499	0.3871	0.8918	0.2831	3.1819	0.9986	3.28E-04	0.0181	0.0228	0.0161	0.1117
	80	0.9999	0.0019	0.0439	0.0798	0.0357	0.1778	0.9987	7.12E-04	0.0267	0.0429	0.0208	0.1495	0.9995	0.0054	0.0735	0.1250	0.0522	0.4952
Thompson	40	0.9990	0.9709	0.9854	0.2931	0.8227	0.0170	0.9998	0.9216	0.9600	0.2783	0.7268	0.0114	0.9973	91.0028	9.5395	8.8423	7.6826	0.0474
	60	0.9988	1.4468	1.2028	0.3100	0.8242	0.0150	0.9991	1.4410	1.2004	0.5896	0.9287	0.0202	0.9976	18.2727	4.2747	4.1951	3.3757	0.0592
	80	0.9997	0.1011	0.3179	0.0927	0.2011	0.0119	0.9986	0.6375	0.7984	0.1549	0.5863	0.0265	0.9992	0.3765	0.6136	0.2359	0.4972	0.0189
Geometric	40	0.9059	0.1195	0.3457	0.3024	0.2064	0.7965	0.8321	0.0367	0.1917	0.1068	0.1042	0.4628	0.8066	0.0458	0.2141	0.1033	0.1048	0.4397
	60	0.8615	0.0245	0.1565	0.0732	0.0979	0.3662	0.8272	0.0267	0.1634	0.0728	0.0994	0.3352	0.8176	0.0360	0.1898	0.0767	0.1261	0.3528
	80	0.9867	0.0011	0.0337	0.0294	0.0303	0.0861	0.9161	0.0055	0.0743	0.0426	0.0631	0.1948	0.9431	0.0044	0.0665	0.0358	0.0549	0.2371
Verma	40	0.9392	8.66E-05	0.0093	0.0065	0.0064	0.0504	0.9097	7.89E-05	0.0089	0.0092	0.0047	0.1605	0.7899	3.66E-04	0.0191	0.0225	0.0170	0.2831
	60	0.9097	1.41E-04	0.0119	0.0094	0.0093	0.0965	0.8770	1.96E-04	0.0140	0.0121	0.0102	0.0662	0.8609	2.97E-04	0.0172	0.0159	0.0126	0.0817
	80	0.8916	5.42E-04	0.0233	0.0143	0.0184	0.0627	0.9717	2.91E-04	0.0171	0.0034	0.0143	0.0649	0.9404	1.31E-04	0.0115	0.0072	0.0096	0.0660
Two-factor	40	0.8391	2.85E-04	0.0169	0.0172	0.0140	0.1107	0.7165	6.75E-04	0.0260	0.0290	0.0202	0.4270	0.8088	3.66E-04	0.0191	0.0205	0.0175	0.2810
	60	0.7814	5.11E-04	0.0226	0.0227	0.0194	0.1926	0.7811	4.77E-04	0.0218	0.0215	0.0172	0.1402	0.8788	2.94E-04	0.0171	0.0138	0.0129	0.0811
	80	0.8639	5.27E-04	0.0230	0.0180	0.0195	0.0614	0.7696	0.0010	0.0313	0.0273	0.0241	0.0934	0.9361	1.28E-04	0.0113	0.0077	0.0096	0.0657
Midilli	40	0.9942		0.0040		0.0032	0.0209	0.9864		0.0022		0.0014	0.0105	0.9871	0.2082	0.4563	1.4577	0.4214	8.3175

(*continued on next page*)

Table 2 (*continued*)

Model	T (°C)	Air flow 1.6 m/s						Air flow 0.8 m/s						no air flow					
		R^2	X^2	SEE	RMSE	MAE	P_0	R^2	X^2	SEE	RMSE	MAE	P_0	R^2	X^2	SEE	RMSE	MAE	P_0
			1.64E-05		1.31E-04				5.06E-06		6.06E-05								
	60	0.9896	2.32E-05	0.0048	6.55E-05	0.0034	0.0255	0.9915	3.58E-05	0.0060	4.97E-05	0.0049	0.0234	0.9927	0.1818	0.4264	1.1322	0.3774	2.7125
	80	0.9537	1.91E-05	0.0044	7.18E-05	0.0035	0.0262	0.7757	1.04E-04	0.0102	1.31E-05	0.0083	0.0690	0.9965	3.60E-06	0.0019	3.17E-05	0.0013	0.0191
Weibull	40	0.8968	0.0103	0.1015	0.2596	0.0921	0.7335	0.8706	6.48E-06	0.0025	7.83E-06	0.0017	0.0147	0.8746	3.20E-05	0.0057	1.60E-05	0.0050	0.0561
	60	0.8569	2.60E-05	0.0051	3.73E-06	0.0038	0.0243	0.8360	3.41E-05	0.0058	3.31E-09	0.0049	0.0256	0.8968	9.73E-06	0.0031	9.97E-06	0.0026	0.0089
	80	0.7210	2.24E-05	0.0047	9.51E-07	0.0038	0.0281	0.4130	1.03E-04	0.0101	1.97E-06	0.0082	0.0689	0.8984	2.74E-06	0.0017	4.56E-06	0.0012	0.0164

R^2: coefficient of determination; X^2: chi-square error; SEE: standard error of estimation; RMSE: root mean square error; MAE: mean absolute error; P_0: relative mean error.

select the best drying conditions.

Fig. 2 shows the average drying rates of the avocado peels dried at three different temperatures and airflows against time. Depending on the drying conditions, the initial drying rate reached the maximum value at 15–30 min. The drying rate declined rapidly after this time. These facts can be due to the rapid evaporation of the surface moisture occurring in the first half hour and, after that, to the evaporation of the internal moisture. The increase in temperature enhanced the drying rate considerably. In fact, without airflow, the drying rate increased by 77.6% when drying at 80 °C compared to drying at 40 °C. Furthermore, a consistent effect was found with the airflow. The highest impact in the drying rate with the airflow was at 40 °C (an increase of 70.4% when using 1.6 m/s of airflow). However, higher increases were also found with the airflow when drying at 60 °C (64.3%) and 80 °C (54.9%). Fig. 2 shows that the samples dried at 80 °C with airflow reached the highest drying rate among all the tested conditions.

Regarding the drying kinetics, Fig. 1 clearly shows two stages of drying. The first one is the most rapid phase and is mostly linear. In this case, the water of the most superficial layers of the avocado by-product is evaporated. The second one is an exponential phase that usually takes longer and occurs when the remaining water content diffuses to the surface. Therefore, the mathematical modelling of the drying curves is important for better control of the drying process and better quality of the avocado peels.

The statistical parameters presented in Table 2, such as R^2, X^2, RMSE, MAE and P_0, were considered to evaluate which model best predicts the drying kinetics of the avocado peel. In general, most of the models provided satisfactory results with a high coefficient of determination ($R^2 > 0.9$). Among the fourteen tested mathematical models, when no airflow was used, the Page, Polynomial and Thompson models fitted the best at all three temperatures showing R^2 values of 0.9907–0.9973, 0.9986–0.9998, and 0.9973–0.9992, respectively. When using airflows of 0.8 or 1.6 m/s, the best model adjustment changed depending on the temperature. At 40 °C and 60 °C, Page, polynomial and Thompson models reported the highest values of R^2, but only Page model kept X^2, SEE, RMSE, MAE and P_0 the lowest. However, at 80 °C, the Lewis model was found to better fit the experimental data with polynomial and Thompson models. Other models such as Verma, Two-factor, Midilli and Weibull did not show good statistical results for the temperatures and air flows tested predicting the drying kinetics of the avocado peel. These results show that the drying kinetics vary depending on the temperature and airflow used when drying avocado peel by convective drying. Additionally, Table 3 shows the values obtained for all the constants of all the models. All these parameters were variable and exhibited temperature and airflow dependence in consistency with other authors (Avhad & Marchetti, 2016; Nguyen & Le, 2022).

The effective moisture diffusivity (D_{eff}) was calculated according to Fick's second law of diffusion for the three different drying temperatures and airflows at all the mathematical models tested, when possible, as some models such as Wang and Singh, Parabolic, Polynomial, Thompson and Geometric did not have kinetic constant (k). The obtained values ranged between 10^{-7} and 10^{-9} m^2/s in consistency with the ranges reported by other authors (Cavalcanti-Mata et al., 2020; Ferreira et al., 2021; Gaikwad et al., 2022; Nguyen & Le, 2022; Sahoo et al., 2022).

The Ea is the required energy for initializing the moisture diffusion from the inside to the outer of the sample. The Ea and the pre-exponential factors for the studied models at the three different airflows were calculated using the Arrhenius equation from the plot of ln (D_{eff}) versus 1/T. Fig. 3 shows an example of this plot for the Page model for the three different airflows. The results are represented in Table 4. The Ea was calculated in the temperature range from 313 to 353 K for all the cases.

For the avocado peel dried with an airflow of 1.6 m/s, 0.8 m/s or without airflow, the Ea values were 2.76–36.56, 1.27–51.37 and 38.74–85.29 kJ/mol, respectively. Nguyen and Le (2022) reported Ea for avocado and mango pulp of 32.06 and 66.03 kJ/mol, respectively,

Table 3
Results of the nondimensional coefficients for the different mathematical models for the avocado peels.

Air flow		1.6 m/s			0.8 m/s			No		
Temperature (°C)		**40**	**60**	**80**	**40**	**60**	**80**	**40**	**60**	**80**
Lewis	k	0.0353	0.0305	0.0565	0.0180	0.0254	0.0448	0.0078	0.0126	0.0504
Henderson and Pabis	k	0.0371	0.0331	0.0582	0.0175	0.0272	0.0468	0.0096	0.0145	0.0529
	a	1.1296	1.2148	1.0625	1.1730	1.1687	1.0952	1.9519	1.3354	1.1192
Page	k	0.0216	0.0145	0.0114	0.0053	0.0153	0.0301	0.0007	0.0014	0.0309
	N	1.1123	1.1635	1.4974	1.2349	1.1056	1.0987	1.3975	1.4202	1.1226
Logarithmic	k	0.0582	0.0331	0.0371	0.0468	0.0272	0.0202	0.0529	0.0145	0.0089
	a	0.7969	0.9111	0.8472	0.8214	0.8765	1.0268	0.8394	1.0015	1.1068
	c	0.2656	0.3037	0.2824	0.2738	0.2922	0.3423	0.2798	0.3338	0.3689
Avhad and Marchetti	k	0.1140	0.0753	0.0228	0.0126	0.0610	0.1161	0.0147	0.0140	0.1584
	a	1.9358	1.8450	0.9008	1.3818	1.6401	1.7620	2.1964	1.5932	2.1615
	n	0.7822	0.8472	1.4974	1.0939	0.8509	0.8174	0.9347	1.0219	0.7789
Wang and Sigh	a	−0.0225	−0.0189	−0.0374	−0.0104	−0.0164	−0.0304	−0.004	−0.0074	−0.0316
	b	1E-04	9E-05	4E-04	3E-05	7E-05	2E-04	4E-06	1E-05	2E-04
Parabolic	a	0.9585	0.9659	0.9814	0.9669	0.9589	0.9756	0.9669	1.0199	0.9652
	b	−0.0211	−0.0179	−0.0363	−0.0098	−0.0153	−0.0291	−0.0098	−0.0077	−0.0299
	c	1E-04	8E-05	3E-04	3E-05	6E-05	2E-04	3E-05	1E-05	2E-04
Polynomial	a	0.9985	0.9999	1.0070	1.0033	0.9937	0.9973	1.0038	1.0139	0.9965
	b	−0.0280	−0.0228	−0.0455	−0.0123	−0.0195	−0.038	−0.004	−0.0073	−0.0395
	c	3E-04	2E-04	8E-04	5E-05	1E-04	6E-04	4E-06	1E-05	6E-04
	d	-1E-06	-6E-07	-5E-06	-8E-08	-4E-07	-4E-06	7E-10	1E-08	−3.00E-06
Thompson	a	−35.12	−44.01	−20.59	−78.93	−50.92	−27.67	−201.21	−118.61	−25.15
	b	−2.540	−4.119	−1.296	−7.151	−4.536	−2.312	−23.01	−16.74	−2.0261
Geometric	a	60.66	71.58	45.31	739.52	48.25	42.68	2287.50	146.12	72.70
	n	1.554	1.537	1.658	1.879	1.373	1.541	1.798	1.385	1.750
Verma	a	13.1485	10.0958	0.8166	6.0032	10.0963	2.4646	11.6018	9.9967	−1.2061
	k1	0.0464	0.0402	0.0537	0.0228	0.0332	0.0260	0.0106	0.0196	0.0772
	k2	0.0480	0.0424	0.0537	0.0253	0.0348	0.0188	0.0115	0.0216	0.0598
Two factor	a	0.8561	0.8491	0.8165	0.8916	0.8308	0.8998	−6.0258	19.5327	−3.0924
	b	0.1563	0.1716	0.1920	0.1386	0.1847	0.1115	7.0192	−18.5368	4.0914
	k1	0.0328	0.0273	0.0540	0.0149	0.0233	0.0436	0.0119	0.0201	0.0705
	k2	0.0328	0.0273	0.0540	0.0149	0.0233	0.0346	0.0104	0.0211	0.0628
Midilli	k	0.0271	0.0202	0.0386	0.0081	0.0206	0.0603	0.0012	0.0021	0.0439
	a	1.0005	1.0008	1.0002	1.0007	0.9985	0.9999	0.9963	1.0016	1.0000
	b	−0.0003	−0.0004	−0.0006	−0.0001	−0.0004	−0.0023	−0.0001	−0.0002	−0.0006
	n	1.0345	1.0548	1.0833	1.1231	1.0021	0.8179	1.2646	1.3165	0.9946
Weibull	k	0.0204	0.0202	0.0390	0.0083	0.0204	0.0494	0.0013	0.0022	0.0442
	a	−0.0824	−0.0538	−0.0443	−0.0326	−0.0824	−0.3612	−0.0717	−0.0706	−0.0565
	b	−1.0812	−1.0547	−1.0444	−1.0334	−1.0812	−1.3612	−1.0684	−1.0724	−1.0565
	n	0.9833	1.0401	1.0655	1.1114	0.9833	0.7831	1.2413	1.2971	0.9732

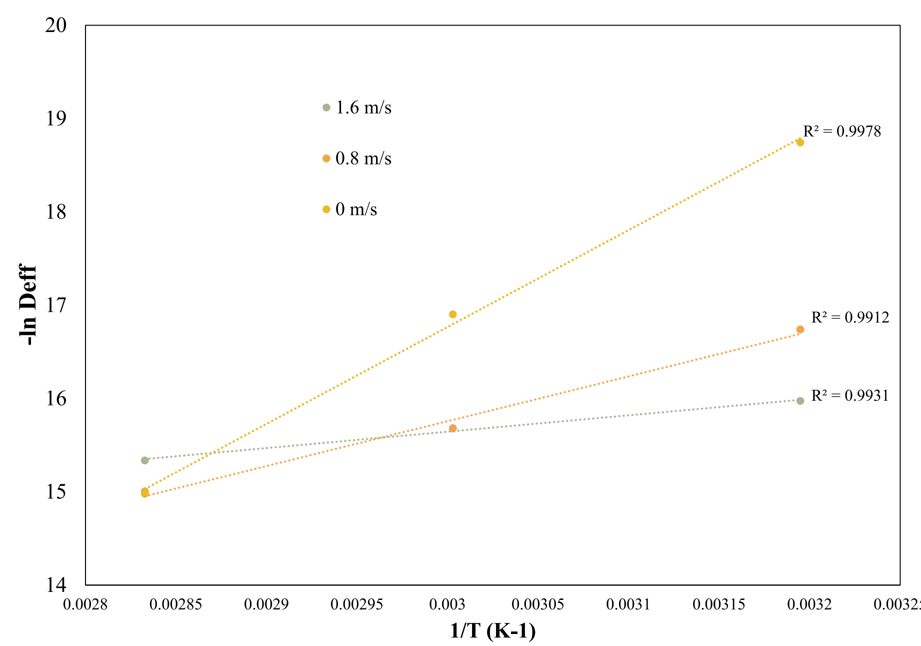

Fig. 3. Relationship between effective moisture diffusivity (D_{eff}) and drying temperatures at the three different airflows according to the Page Model.

Table 4
Estimated activation energy (Ea) and pre-exponential factor (A) for avocado peels dried with different airflows in the temperature range 313–353 K.

Model	Air flow 1.6 m/s		Air flow 0.8 m/s		No air flow	
	Ea (kJ/mol)	A	Ea (kJ/mol)	A	Ea (kJ/mol)	A
Lewis	10.44	2.29E+05	20.81	7.70E+03	42.38	5.02
Henderson and Pabis	10.02	2.53E+05	22.52	4.04E+03	38.74	16.42
Page	14.69	5.28E+09	39.95	15.31	85.29	4.82E-06
Logarithmic	10.02	2.53E+05	19.16	1.30E+04	40.51	8.87
Avhad and Marchetti	36.56	3.81E+12	51.37	13.52	53.39	20.13
Midilli	7.68	8.86E+05	45.93	1.10	80.93	1.54E-05
Weibull	14.51	8.16E+04	41.01	6.94	79.61	2.39E-05
Verma	2.76	1.54E+06	1.27	1.12E+07	41.55	0.43
Two factor	11.06	9.90E+04	22.09	2.79E+03	40.75	3.11

drying by refractance window drying at 80–90 °C. Moreover, the results were consistent with those reported for other matrices (Cavalcanti-Mata et al., 2020; Llavata et al., 2022; Nguyen & Le, 2022; Sahoo et al., 2022). It is clear from the results that higher Ea is necessary when drying without airflow; in contrast, the Ea needed to start the moisture diffusion is lower if the airflow is introduced. The highest Ea values were obtained with Avhad and Marchetti's model when drying with airflow and with Page's model when no airflow was used. Among all the models, the Verma model predicted the lowest Ea when using an airflow of 1.6 and 0.8 m/s, and the Henderson and Pabis model then drying without air flow.

3.2. *Effect of drying on procyanidin content determined using HPLC-FLD*

Procyanidins are valuable and thermolabile compounds of great interest, and they are present in the avocado by-products that could be exploited and revalued. Therefore, the procyanidin contents of the samples dried at 40, 60 and 80 °C at three different airflows were evaluated after the extraction. Ultrasound technology was used, allowing the extraction of the highest possible content of bioactive compounds without using high temperatures (Díaz-de-Cerio et al., 2017; Martín-García et al., 2021; Razola-Díaz et al., 2021). Procyanidin content was determined using HPLC-FLD. Table 5 shows the procyanidin contents obtained. Procyanidins are ordered according to their polymerization degree (dp2-dp8), including the sum of monomers (catechin + epicatechin) and the rest of polymers with a polymerization degree above 8.

The results show the huge impact of temperature and airflow on total procyanidin content in the avocado by-product, ranging from 1765.54 to 4225.96 μg CE/g d.w. To our knowledge, no previous references about the evaluation of the drying conditions among the procyanidin content of avocado peel are available. However, previously, López-Cobo et al. (2016) have reported the procyanidin content of avocado peels measured using HPLC-FLD, and the profile distribution reported in the present study is consistent with them. Other authors have also reported similar procyanidin profiles measured in hawthorn (Pavlovic et al., 2019) and cranberries (Vidal-Casanella et al., 2022) using HPLC-FLD.

The highest procyanidin retention was found at 80 °C when the samples were dried without airflow, mainly due to the reduced time needed to reach the final moisture content. However, differences in this tendency were found when considering the effect of the airflow. When airflow increased, an increase in procyanidin content was found at 40 and 60 °C but occurred the opposite at 80 °C. It is mainly attributable to the case-hardening effect occurring at the highest temperatures, promoted by the airflow and entailing a decrease in the procyanidin content. The procyanidin content decreased to 1784.40 μg CE/g d.w. when drying at 80 °C and airflow of 1.6 m/s for 60 min, very similar to the result obtained when drying at 40 °C without airflow for 480 min. If comparing the total procyanidin content at 60 °C with airflow of 1.6 m/s (2747.9 μg CE/g d.w.) and at 80 °C without airflow (2708.97 μg CE/g d.w.), as no significant differences were found between the results ($p > 0.05$), probably the selected drying conditions would be those at 80 °C because the time needed was 37.5% lower. However, the highest procyanidin content in all cases was obtained when drying at 40 °C with airflow of 1.6 m/s for 105 min. Even though the time required is 43% higher than at 80 °C without airflow, the increase in total procyanidin content is 36%. Wojdyło et al. (2016) reported that total flavan-3-ols content decreased when drying jujube fruits at an airflow of 1 m/s and increasing the temperature from 50 to 70 °C. Szychowski et al. (2018) also reported decreased total procyanidin content with the convective drying temperature in quinces. Similarly, Donlao and Ogawa (2019) reported a decrease in the total procyanidin content of green tea leaves when the convective drying temperature increased from 80 to 160 °C. In the present study, we found similar decreases in the total

Table 5
Procyanidin content of the avocado peels dried at different temperatures and airflows measured using high-performance liquid chromatography with a fluorometric detector (HPLC-FLD). Procyanidin content is expressed as μg Catechin Equivalents (CE)/g dry weight (d.w.).

	40 °C	40 °C 0.8 m/s	40 °C 1.6 m/s	60 °C	60 °C 0.8 m/s	60 °C 1.6 m/s	80 °C	80 °C 0.8 m/s	80 °C 1.6 m/s
Monomers	1045.07 ± 6.68 e	1300.15 ± 8.21 a	1274.12 ± 7.58 a,b	1098.53 ± 5.47 d	1110.02 ± 5.11 d	1188.64 ± 8.33 c	1255.05 ± 7.80 b	1167.43 ± 5.47 c	1105.03 ± 5.55 d
Dimers	208.97 ± 5.90 c	704.97 ± 19.99 a	752.88 ± 21.78 a	219.39 ± 6.67 c	391.90 ± 12.15 b	464.01 ± 12.66 b	419.35 ± 11.96 b	432.38 ± 13.35 b	201.21 ± 6.11 c
dp3	140.56 ± 3.16 e	703.91 ± 15.92 a	745.11 ± 17.25 a	240.75 ± 5.91 d	389.35 ± 9.77 c	451.96 ± 9.77 b	404.48 ± 9.21 b,c	397.81 ± 9.94 b,c	190.79 ± 4.67 d,e
dp4	153.49 ± 5.33 c	438.36 ± 15.28 a	475.38 ± 16.86 a	172.72 ± 6.40 c	264.85 ± 9.98 b	289.96 ± 9.78 b	262.45 ± 9.19 b	258.32 ± 9.69 b	132.20 ± 4.89 c
dp5	88.94 ± 3.57 d	249.88 ± 10.07 b	289.97 ± 11.87 a	97.72 ± 4.16 d	152.49 ± 6.60 c	160.20 ± 6.27 c	152.59 ± 6.18 c	144.60 ± 6.24 c	73.03 ± 3.11 d
dp6	36.08 ± 2.61 b,c	105.00 ± 7.60 a	131.07 ± 9.59 a	39.48 ± 2.97 b,c	66.27 ± 5.05 b	66.04 ± 4.68 b	65.96 ± 4.79 b	62.77 ± 4.77 b	32.08 ± 2.41 c
dp7	24.28 ± 0.80 d	83.19 ± 2.76 b	110.40 ± 3.73 a	26.53 ± 0.94 d	46.73 ± 1.68 c	47.07 ± 1.51 c	50.80 ± 1.69 c	45.90 ± 1.64 c	20.31 ± 0.72 d
dp8	6.31 ± 0.33 d	36.27 ± 1.93 b	53.78 ± 2.90 a	6.75 ± 0.38 d	15.11 ± 0.85 c	16.53 ± 0.86 c	19.27 ± 1.03 c	15.76 ± 0.89 c	3.69 ± 0.21 d
Polymers	61.84 ± 4.47 c	225.69 ± 16.34 b	349.74 ± 25.60 a	55.30 ± 4.17 c	57.39 ± 4.37 c	60.19 ± 4.26 c	75.37 ± 5.47 c	45.59 ± 3.47 c	26.06 ± 1.96 c
Total procyanidins	1765.54 ± 32.86 c	3867.07 ± 98.09 a	4225.96 ± 117.15 a	1957.17 ± 37.07 c	2496.46 ± 55.56 b	2747.95 ± 58.11 b	2708.97 ± 57.32 b	2570.55 ± 55.45 b	1784.40 ± 29.62 c

dp: polymerization degree. Different letters (a-e) in the same row indicate significant differences ($p < 0.05$).

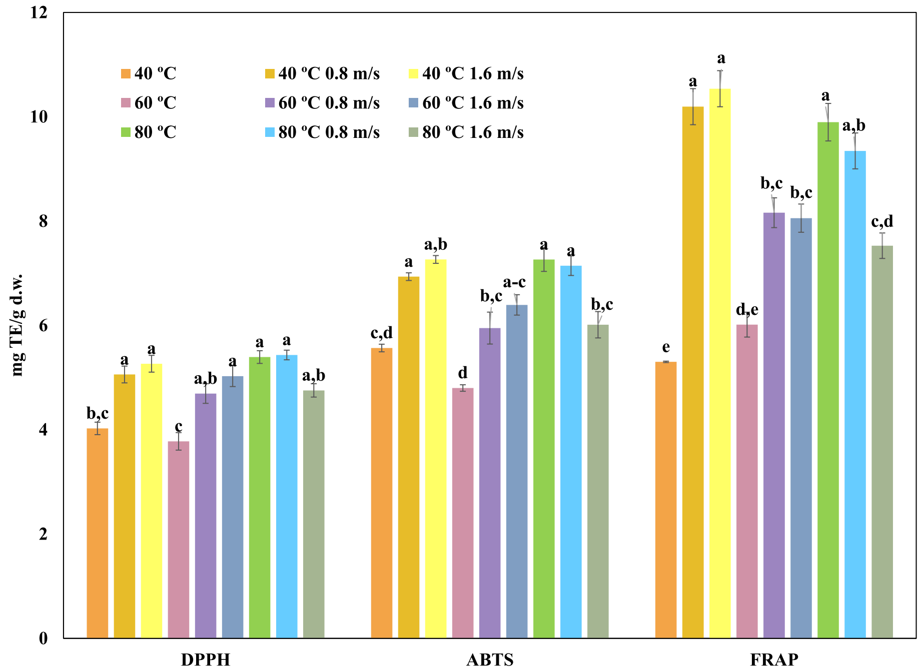

Fig. 4. Antioxidant activity measured using DPPH, ABTS and FRAP methods of the avocado by-product dried by convective drying at different temperatures and airflows. The results are expressed as mg Trolox equivalents (TE)/g dry weight (d.w.) Different letters (a–e) for the same method indicate significant differences ($p < 0.05$).

flavan-3-ol content when increasing the drying temperature from 40 to 60 °C with airflows of 0.8 or 1.6 m/s.

Furthermore, according to Liu et al. (2021), convective drying maintains or increases the procyanidins degree of polymerization in strawberries, apple pomaces, and grapes. In our cases, we found no changes in the degree of polymerization, but it was maintained among the temperatures and airflows tested.

3.3. *Effect of drying on the antioxidant activity*

The antioxidant activity was measured using three different methods to select the best convective drying conditions in terms of temperature and airflow. Fig. 4 shows the results obtained in the avocado peel by-products dried at 40, 60 and 80 °C with an airflow of 0.8 m/s or 1.6 m/s or without airflow for the three antioxidant assays performed. The results ranged from 3.78 ± 0.17 to 5.43 ± 0.09 mg TE/g d.w. for the DPPH, from 4.80 ± 0.06 to 7.26 ± 0.07 mg TE/g d.w. for the ABTS method, and from 5.30 ± 0.14 to 10.54 ± 0.46 mg TE/g d.w. for FRAP. Temperature and airflow also have shown an important influence on the antioxidant activity of the avocado by-product. When drying without airflow at high temperatures (80 °C), the samples exhibited higher antioxidant activity than at lower temperatures (60 and 40 °C), in consistency with the reported by Vega-Gálvez et al. (2009) for red peppers. According to these authors, this behaviour is explained because the drying process at low temperatures implies longer drying times that clearly promote a decrease in antioxidant activity. Moreover, it could also be explained by the generation and accumulation of Maillard compounds at higher temperatures that could enhance the antioxidant properties. Llavata et al. (2022) reported consistent results, with values of 28, 30 and 35 mg/kg d.w., determined using FRAP when drying cider apple pomace at 40, 60 and 80 °C, respectively. In the same way as the procyanidin content, at 80 °C the antioxidant activity decreases when increasing the airflow. In contrast, at 60 °C with 1.6 m/s of airflow, the samples showed 25% higher antioxidant activity by the three methods than without airflow. For the DPPH and ABTS methods, the results obtained when drying at 40 °C and 1.6 m/s and 80 °C without airflow showed no significant differences ($p < 0.05$).

Previously some authors have evaluated the effect of drying on the antioxidant activities of avocado matrices. Saavedra et al. (2017) reported 5180.81 mg GAE/100 g d.w. by using DPPH in avocado peel dried at its optimal conditions of 72.71 °C and 0.8 m/s of airflow. In seeds drying at 65.52 °C and 1.39 m/s, the result obtained was 4132.7 mg GAE/g d.w. In avocado leaves, Loh and Lim (2018) reported values of 7.17 and 8.47 mg GAE/g d.w. using the FRAP assay when dried in an oven at 50 °C and air dried, respectively, and completely in the same magnitude range as our results. Yamassaki et al. (2017), when drying at 40, 60 and 90 °C, reported IC_{50} DPPH values of 53.4, 53.4 and 106.7 μg/mL in avocado leaves, respectively. Our IC_{50} DPPH values were 66.10, 64.25 and 86.54 μg/mL in the avocado peel samples dried at 40, 60 and 80 °C without airflow, respectively. Babiker et al. (2021) reported values of 53.89, 79.21 and 76.73 μg/mL in avocado pulp, peel and seed, respectively, when drying in oven at 60 °C for 19 h.

4. Conclusions

The drying step is essential for storing this avocado by-product at the industrial level to take advantage of it. Therefore, the convective drying of the avocado peel by-product has been studied at three different temperatures (40, 60 and 80 °C) and airflows (0, 0.8 and 1.6 m/s). All these parameters directly influence the time needed to reach a final moisture content below 10%. In addition, the fourteen tested mathematical models for fitting the drying kinetics of the avocado by-product demonstrated satisfactory results. However, the Page model provided better adjustment reporting higher coefficient of regressions and lower square and absolute errors for most of the temperatures and airflows tested. To understand well the behaviour of the avocado peel during drying by using the Page equation will allow us to maximize its exploitation, reducing economic and energy costs. However, this model could be useless for drying the avocado peel using other techniques. Moreover, the procyanidin content determined using HPLC-FLD and the antioxidant activity determined using DPPH, ABTS and FRAP were evaluated to select the better drying conditions. In all cases, both the temperature and the airflow have proven to have a huge influence. The time needed to reach the final moisture content decreased when the airflow increased; therefore, the exposure to temperature is reduced, and consequently, the decrease in procyanidin and antioxidant compounds content is lower. However, the case-hardening phenomenon increased at 80 °C when increasing the airflow, decreasing thus the bioactive content. Finally, taking everything into account, the drying conditions of choice are 40 °C, an airflow of 1.6 m/s for 105 min, which allowed the lowest decrease in flavan-3-ols content and antioxidant activity. The main limitation of these drying conditions is that they could vary slightly depending on the oven size and the by-product itself, which could have different moisture content depending on the avocado growing location and the company processing it. However, convective drying at the optimised conditions would be a beneficial and low-time-consuming drying method for the avocado by-product from guacamole factories in the south of Spain. Finally, this could be scaled up to pilot and industrial scale to obtain dry avocado by-products that could be used as functional ingredients for food, feed and cosmeceutical uses.

Funding

This study was supported by project RTI2018-099835-A-I00 financed by MCIN/AEI/10.13039/501100011033/FEDER "Una manera de hacer Europa", and by the project Proyectos I + D + i del Programa Operativo FEDER 2020 cod. B-AGR-506-UGR20.

CRediT authorship contribution statement

María del Carmen Razola-Díaz: Data curation, Formal analysis, Writing – original draft. **Eduardo Jesús Guerra-Hernández:** Supervision, Conceptualization, Writing – review & editing. **Ana María Gómez-Caravaca:** Data curation, Funding acquisition, Writing – review & editing. **Belén García-Villanova:** Writing – review & editing. **Vito Verardo:** Supervision, Data curation, Funding acquisition, Conceptualization, Writing – review & editing.

Declaration of competing interest

The authors declare that they have no known competing financial interests or personal relationships that could have appeared to influence the work reported in this paper.

Data availability

The authors do not have permission to share data.

Acknowledgments

This paper and the results presented constitute part of María del Carmen Razola-Díaz's Doctoral Thesis performed within the Nutrition and Food Science Doctorate Program of the University of Granada. This author was supported by a Research Fellowship from the Government of Spain (FPU19/02009). The authors thank Nutraceutical Translations for the English language editing of this manuscript. Funding for open access charge: Universidad de Granada / CBUA

References

Alkaltham, M. S., Uslu, N., Özcan, M. M., Salamatullah, A. M., Mohamed Ahmed, I. A., & Hayat, K. (2021). Effect of drying process on oil, phenolic composition and antioxidant activity of avocado (cv. Hass) fruits harvested at two different maturity stages. *LWT - Food Science and Technology, 148*(May). https://doi.org/10.1016/j.lwt.2021.111716

An, N., nan Sun, W., hong, L., zheng, B., Wang, Y., Shang, N., qiao, L. W., Li, D., & Wang, L. jun (2022). Effect of different drying techniques on drying kinetics, nutritional components, antioxidant capacity, physical properties and microstructure of edamame. *Food Chemistry, 373*(PB), Article 131412. https://doi.org/10.1016/j.foodchem.2021.131412

Araújo, R. G., Rodriguez-Jasso, R. M., Ruiz, H. A., Pintado, M. M. E., & Aguilar, C. N. (2018). Avocado by-products: Nutritional and functional properties. *Trends in Food Science & Technology, 80*(July), 51–60. https://doi.org/10.1016/j.tifs.2018.07.027

Avhad, M. R., & Marchetti, J. M. (2016). Mathematical modelling of the drying kinetics of Hass avocado seeds. *Industrial Crops and Products, 91*, 76–87. https://doi.org/10.1016/j.indcrop.2016.06.035

Babiker, E. E., Mohamed Ahmed, I. A., Uslu, N., Özcan, M. M., Al Juhaimi, F., Ghafoor, K., & Almusallam, I. A. (2021). Influence of drying methods on bioactive properties, fatty acids and phenolic compounds of different parts of ripe and unripe avocado fruits. *Journal of Oleo Science, 70*(4), 589–598. https://doi.org/10.5650/jos.ess20343

Berbert, P. A., Oliveira, M. T. R. de, Molina, M. A. B., Soares, K. de J., & Coelho, A. A. (2019). Thin-layer convective drying behaviour of brazilian peppertree leaves TT - secagem em camada delgada de folhas de aroeira. *Bioscience Journal, 35*(2), 540–560. http://www.seer.ufu.br/index.php/biosciencejournal/article/view/42203/25806%0Ahttp://fi-admin.bvsalud.org/document/view/v52m2.

Brand-Williams, W., Cuvelier, M. E., & Berset, C. (1995). Use of a free redical method to evaluate antioxidant activity. *LWT - Food Science and Technology, 28*, 25–30.

de Brito Araújo, A. J., da Silva, W. P., dos Santos Moreira, I., & Santos, N. C. (2021). Effect of drying temperature on the physicochemical characteristics, bioactive compounds, and antioxidant activity of "Palmer" mango peels. *Journal of Food Process Engineering, 44*(11). https://doi.org/10.1111/jfpe.13860

Castro, A. M., Mayorga, E. Y., & Moreno, F. L. (2018). Mathematical modelling of convective drying of fruits: A review. *Journal of Food Engineering, 223*, 152–167. https://doi.org/10.1016/j.jfoodeng.2017.12.012

Cavalcanti-Mata, M. E. R. M., Duarte, M. E. M., Lira, V. V., Oliveira, R. F., Costa, N. L., & Oliveira, H. M. L. (2020). A new approach to the traditional drying models for the thin-layer drying kinetics of chickpeas. *Journal of Food Process Engineering, 43*(12), Article e13569. https://doi.org/10.1111/jfpe.13569

Colombo, R., & Papetti, A. (2019). Avocado (Persea americana mill.) by-products and their impact: From bioactive compounds to biomass energy and sorbent material for removing contaminants. A review. *International Journal of Food Science and Technology, 54*(4), 943–951. https://doi.org/10.1111/ijfs.14143

Corrêa, P. C., Baptestini, F. M., Zeymer, J. S., de Araujo, M. E. V., de Freitas, R. C. P., & Leite, R. A. (2019). Dehydration of infrared ginger slices: Heat and mass transfer coefficient and modeling. *Ciencia E Agrotecnologia, 43*. https://doi.org/10.1590/1413-7054201943025318

Deng, L., Mujumdar, A. S., Yang, W., Zhang, Q., Zheng, Z., Wu, M., & Xiao, H. (2020). Hot air impingement drying kinetics and quality attributes of orange peel. *Journal of Food Processing and Preservation, 44*(1), 1–11. https://doi.org/10.1111/jfpp.14294

Díaz-de-Cerio, E., Tylewicz, U., Verardo, V., Fernández-Gutiérrez, A., Segura-Carretero, A., & Romani, S. (2017). Design of sonotrode ultrasound-assisted extraction of phenolic compounds from psidium guajava L. Leaves. *Food Analytical Methods, 10*(8), 2781–2791. https://doi.org/10.1007/s12161-017-0836-z

Dikmen, E., Ayaz, M., Kovacı, T., & Şahin, A.Ş. (2019). Mathematical modelling of drying characteristics of medical plants in a vacuum heat pump dryer. *International Journal of Ambient Energy, 40*(6), 616–623. https://doi.org/10.1080/01430750.2017.1423383

Donlao, N., & Ogawa, Y. (2019). The influence of processing conditions on catechin, caffeine and chlorophyll contents of green tea (*Camelia sinensis*) leaves and infusions. *LWT–Food Science and Technology, 116*, Article 108567. https://doi.org/10.1016/j.lwt.2019.108567

Falade, K. O., & Solademi, O. J. (2010). Modelling of air drying of fresh and blanched sweet potato slices. *International Journal of Food Science and Technology, 45*(2), 278–288. https://doi.org/10.1111/j.1365-2621.2009.02133.x

Ferreira, J. P. de L., Queiroz, A. J. de M., Figueirêdo, R. M. F. de, Silva, W. P. da, Gomes, J. P., Santos, D. da C., Silva, H. A., Rocha, A. P. T., Paiva, A. C. C. de, Chaves, A. D. C. G., Lima, A. G. B. de, & Andrade, R. O. de (2021). Utilization of Cumbeba (*Tacinga inamoena*) residue: Drying kinetics and effect of process conditions on antioxidant bioactive compounds. *Foods, 10*(4), 788. https://doi.org/10.3390/foods10040788

Figueroa, J. G., Borrás-Linares, I., Lozano-Sánchez, J., Quirantes-Piné, R., & Segura-Carretero, A. (2018). Optimization of drying process and pressurized liquid extraction for recovery of bioactive compounds from avocado peel by-product. *Electrophoresis, 39*(15), 1908–1916. https://doi.org/10.1002/elps.201700379

Gaikwad, P. S., Sunil, C. K., Negi, A., & Pare, A. (2022). Effect of microwave assisted hot-air drying temperatures on drying kinetics of dried black gram papad (Indian snack food). *Applied Food Research, 2*(2), Article 100144. https://doi.org/10.1016/j.afres.2022.100144

García-Vargas, M. C., Contreras, M. D. M., & Castro, E. (2020). Avocado-derived biomass as a source of bioenergy and bioproducts. *Applied Sciences, 10*(22), 1–29. https://doi.org/10.3390/app10228195

Ghodake, H. M., Goswami, T. K., & Chakraverty, A. (2006). Mathematical modeling of withering characteristics of tea leaves. *Drying Technology, 24*(2), 159–164. https://doi.org/10.1080/07373930600558979

Gomes, B.d. O., Costa Santos, K., Reis Carvalho, G., Sousa Bitencourt, B., Souza Guedes, J., & Duarte, P. E. (2022). Uvaia fruit (*Eugenia pyriformis* Cambess) drying: Ethanol as pre-treatment, convective drying kinetics and bioactive compounds. *Journal of Food Processing and Preservation, 46*(2), Article e16284. https://doi.org/10.1111/jfpp.16284

Górnicki, K., Kaleta, A., & Choińska, A. (2020). Suitable model for thin-layer drying of root vegetables and onion. *International Agrophysics, 34*(1), 79–86. https://doi.org/10.31545/intagr/115190

Haghi, A. K., & Ghanadzadeh, H. (2005). A study of thermal drying process. *Indian Journal of Chemical Technology, 12*(6), 654–663.

Henderson, S. M. (1961). Grain drying theory (I) temperature effect on drying coefficient. *Journal of Agricultural Engineering Research, 6*, 169–174.

Jimenez, P., Garcia, P., Quitral, V., Vasquez, K., Parra-Ruiz, C., Reyes-Farias, M., Garcia-Diaz, D. F., Robert, P., Encina, C., & Soto-Covasich, J. (2021). Pulp, leaf, peel and seed of avocado fruit: A review of bioactive compounds and healthy benefits. *Food Reviews International, 37*(6), 619–655. https://doi.org/10.1080/87559129.2020.1717520

Joseph Bassey, E., Cheng, J., & Sun, D. (2022). Improving drying kinetics, physicochemical properties and bioactive compounds of red dragon fruit (Hylocereus species) by novel infrared drying. *Food Chemistry, 375*, Article 131886. https://doi.org/10.1016/j.foodchem.2021.131886. December 2021.

Karathanos, V. T., & Belessiotis, V. G. (1999). Application of a thin-layer equation to drying data of fresh and semi-dried fruits. *Journal of Agricultural Engineering Research, 74*(4), 355–361. https://doi.org/10.1006/jaer.1999.0473

Kohli, D., Champawat, P. S., Jain, S. K., Mudgal, V. D., & Shahi, N. C. (2022). Mathematical modelling for drying kinetics of asparagus roots (*Asparagus racemosus* L.) and determination of energy consumption. *Biointerface Research in Applied Chemistry, 12*(3), 3572–3589. https://doi.org/10.33263/BRIAC123.35723589

Lewis, W. K. (1921). The rate of drying of solid materials. *Journal of Industrial and Engineering Chemistry, 13*(5), 427–432. https://doi.org/10.1021/ie50137a021

Liu, X., Le Bourvellec, C., Guyot, S., & Renard, C. M. G. C. (2021). Reactivity of flavanols: Their fate in physical food processing and recent advances in their analysis by depolymerization. *Comprehensive Reviews in Food Science and Food Safety, 20*(5), 4841–4880. https://doi.org/10.1111/1541-4337.12797

Llavata, B., Picinelli, A., Simal, S., & Cárcel, J. A. (2022). Cider apple pomace as a source of nutrients: Evaluation of the polyphenolic profile, antioxidant and fiber properties after drying process at different temperatures. *Food Chemistry X, 15*(July), Article 100403. https://doi.org/10.1016/j.fochx.2022.100403

Loh, Z. H., & Lim, Y. Y. (2018). Drying effects on antioxidant activity, enzyme activity, and phytochemicals of avocado (Persea americana) leaves. *Journal of Food Processing and Preservation, 42*(10), 1–11. https://doi.org/10.1111/jfpp.13667

López-Cobo, A., Gómez-Caravaca, A. M., Pasini, F., Caboni, M. F., Segura-Carretero, A., & Fernández-Gutiérrez, A. (2016). HPLC-DAD-ESI-QTOF-MS and HPLC-FLD-MS as valuable tools for the determination of phenolic and other polar compounds in the edible part and by-products of avocado. *LWT - Food Science and Technology, 73*, 505–513. https://doi.org/10.1016/j.lwt.2016.06.049

Martín-García, B., Razola-Díaz, M. D. C., Gómez-Caravaca, A. M., Benítez, G., & Verardo, V. (2021). Setup of an ultrasonic-assisted extraction to obtain high phenolic recovery in crataegus monogyna leaves. *Molecules, 26*(15), 1–16. https://doi.org/10.3390/molecules26154536

McMinn, W. A. M., & Magee, T. R. A. (1999). Principles, methods and applications of the convective drying of foodstuffs. *Food and Bioproducts Processing: Transactions of the Institution of of Chemical Engineers, Part C, 77*(3), 175–193. https://doi.org/10.1205/096030899532466

Nguyen, H. Le, & Le, T. Q. (2022). Drying kinetics and effective moisture diffusivity of pomelo albedo under vacuum-assisted microwave drying and its semi-product. *Journal of Food Process Engineering*, 1–12. https://doi.org/10.1111/jfpe.13968. November 2021.

Nguyen, T. V. L., Nguyen, Q. D., & Nguyen, P. B. D. (2022). Drying kinetics and changes of total phenolic content, antioxidant activity and color parameters of mango and avocado pulp in refractance window drying. *Polish Journal of Food and Nutrition Sciences, 72*(1), 27–38. https://doi.org/10.31883/pjfns/144835

Ozarslan, R., & Bas, E. (2020). Kinetic model for drying in frame of generalized fractional derivatives. *Fractal and Fractional, 4*(2), 1–12. https://doi.org/10.3390/fractalfract4020017

Özbek, H. N., Koç, B., Koçak Yanık, D., & Göğüş, F. (2022). Hot air-assisted radiofrequency drying of avocado: Drying behavior and the associated effect on the characteristics of avocado powder. *Journal of Food Process Engineering, 45*(9), 1–11. https://doi.org/10.1111/jfpe.14094

Parejo, I., Codina, C., Petrakis, C., & Kefalas, P. (2000). Evaluation of scavenging activity assessed by Co(II)/EDTA-induced luminol chemiluminescence and DPPH· (2,2-diphenyl-1-picrylhydrazyl) free radical assay. *Journal of Pharmacological and Toxicological Methods, 44*(3), 507–512. https://doi.org/10.1016/S1056-8719(01)00110-1

Pavlovic, J., Mitic, S., Mitic, M., Kocic, G., Pavlovic, A., & Tosic, S. (2019). Variation in the phenolic compounds profile and antioxidant activity in different parts of hawthorn (crataegus pentagyna willd.) during harvest periods. *Polish Journal of Food and Nutrition Sciences, 69*(4), 367–378. https://doi.org/10.31883/PJFNS/112019

Penteado-Rosa, D., Cantú-Lozano, D., Luna-Solano, G., Polachini, T. C., & Telis-Romero, J. (2015). Modelagem matemática da cinética de secagem de semente de laranja. *Ciencia E Agrotecnologia, 39*(3), 291–300. https://doi.org/10.1590/S1413-70542015000300011

Pulido, R., Bravo, L., & Saura-Calixto, F. (2000). Antioxidant activity of dietary polyphenols as determined by a modified ferric reducing/antioxidant power assay. *Journal of Agricultural and Food Chemistry, 48*(8), 3396–3402. https://doi.org/10.1021/jf9913458

Razola-Díaz, M., del, C., Guerra-Hernández, E. J., Rodríguez-Pérez, C., Gómez-Caravaca, A. M., García-Villanova, B., & Verardo, V. (2021). Optimization of ultrasound-assisted extraction via sonotrode of phenolic compounds from orange by-products. *Foods, 10*(5), 1120. https://doi.org/10.3390/foods10051120

Re, R., Pellegrini, N., Proteggente, A., Pannala, A., Yang, M., & Rice-Evans, C. (1999). Antioxidant activity applying an improved ABTS radical cation decolorization assay. *Free Radical Biology & Medicine, 26*, 1231–1237.

Robbins, R. J., Leonczak, J., Johnson, J. C., Li, J., Kwik-Uribe, C., Prior, R. L., & Gu, L. (2009). Method performance and multi-laboratory assessment of a normal phase high pressure liquid chromatography-fluorescence detection method for the quantitation of flavanols and procyanidins in cocoa and chocolate containing samples. *Journal of Chromatography A, 1216*(24), 4831–4840. https://doi.org/10.1016/j.chroma.2009.04.006

Saavedra, J., Córdova, A., Navarro, R., Díaz-Calderón, P., Fuentealba, C., Astudillo-Castro, C., Toledo, L., Enrione, J., & Galvez, L. (2017). Industrial avocado waste: Functional compounds preservation by convective drying process. *Journal of Food Engineering, 198*, 81–90. https://doi.org/10.1016/j.jfoodeng.2016.11.018

Sahoo, M., Titikshya, S., Aradwad, P., Kumar, V., & Naik, S. N. (2022). Study of the drying behaviour and color kinetics of convective drying of yam (Dioscorea hispida) slices. *Industrial Crops and Products, 176*, Article 114258. https://doi.org/10.1016/j.indcrop.2021.114258. November 2021.

Shen, L., Zhu, Y., Liu, C., Wang, L., Liu, H., Kamruzzaman, M., Liu, C., Zhang, Y., & Zheng, X. (2020). Modelling of moving drying process and analysis of drying characteristics for germinated brown rice under continuous microwave drying. *Biosystems Engineering, 195*, 64–88. https://doi.org/10.1016/j.biosystemseng.2020.05.002. June.

Statista. (2022). The Statistics portal for Market data, Market research and Market Studies. n.d.). Retrieved May 18 https://www.statista.com/.

Szychowski, P. J., Lech, K., Sendra-Nadal, E., Hernández, F., Figiel, A., Wojdyło, A., & Carbonell-Barrachina, Á. A. (2018). Kinetics, biocompounds, antioxidant activity, and sensory attributes of quinces as affected by drying method. *Food Chemistry, 255*, 157–164. https://doi.org/10.1016/J.FOODCHEM.2018.02.075

Taylor, J. (1997). *Introduction to error analysis, the study of uncertainties in physical measurements* (2nd ed.).

Togrul, I. T., & Pehlivan, D. (2002). Mathematical modelling of solar drying of apricots in thin layers. *Journal of Food Engineering, 55*(3), 209–216. https://doi.org/10.1016/S0260-8774(02)00065-1

Vega-Gálvez, A., Di Scala, K., Rodríguez, K., Lemus-Mondaca, R., Miranda, M., López, J., & Perez-Won, M. (2009). Effect of air-drying temperature on physico-chemical properties, antioxidant capacity, colour and total phenolic content of red pepper (*Capsicum annuum*, L. var. Hungarian). *Food Chemistry, 117*(4), 647–653. https://doi.org/10.1016/j.foodchem.2009.04.066

Vega-Gálvez, A., Miranda, M., Díaz, L. P., Lopez, L., Rodriguez, K., & Scala, K. Di (2010). Effective moisture diffusivity determination and mathematical modelling of the drying curves of the olive-waste cake. *Bioresource Technology, 101*(19), 7265–7270. https://doi.org/10.1016/j.biortech.2010.04.040

Vidal-Casanella, O., Arias-Alpizar, K., Núñez, O., & Saurina, J. (2022). Extraction and characterization of flavanol-rich nutraceuticals based on high-performance liquid chromatography. *Separations, 9*(4), 87. https://doi.org/10.3390/separations9040087

Wang, C. Y., & Singh, R. P. (1978). *Use of variable equilibrium moisture content in modelling rice drying.* Paper - American Society of Agricultural Engineers.

Wojdyło, A., Figiel, A., Legua, P., Lech, K., Carbonell-Barrachina, Á. A., & Hernández, F. (2016). Chemical composition, antioxidant capacity, and sensory quality of dried jujube fruits as affected by cultivar and drying method. *Food Chemistry, 207*, 170–179. https://doi.org/10.1016/J.FOODCHEM.2016.03.099

Xu, H., Wu, M., Wang, Y., Wei, W., Sun, D., Li, D., Zheng, Z., & Gao, F. (2022). Effect of combined infrared and hot air drying strategies on the quality of Chrysanthemum (Chrysanthemum morifolium ramat.) cakes: Drying behavior, aroma profiles and phenolic compounds. *Foods, 11*(15), 2240. https://doi.org/10.3390/foods11152240

Yaldýz, O., & Ertekýn, C. (2001). Thin layer solar drying of some vegetables. *Drying Technology, 19*(3–4), 583–597. https://doi.org/10.1081/DRT-100103936

Yamassaki, F. T., Campestrini, L. H., Zawadzki-Baggio, S. F., & Maurer, J. B. B. (2017). Avocado leaves: Influence of drying process, thermal incubation, and storage conditions on preservation of polyphenolic compounds and antioxidant activity. *International Journal of Food Properties, 20*(2), 2280–2293. https://doi.org/10.1080/10942912.2017.1369105

Yang, C. Y., Fon, D. S., & Lin, T. T. (2007). Simulation and validation of thin layer models for peanut drying. *Drying Technology, 25*(9), 1515–1526. https://doi.org/10.1080/07373930701537278

Zhao, T., Dong, Q., Zhou, H., & Yang, H. (2022). Drying kinetics, physicochemical properties, antioxidant activity and antidiabetic potential of *Sargassum fusiforme* processed under four drying techniques. *LWT–Food Science and Technology, 163*, Article 113578. https://doi.org/10.1016/j.lwt.2022.113578. May.

Zhu, X., Zhang, Z., Hinds, L. M., Sun, D. W., & Tiwari, B. K. (2021). Applications of ultrasound to enhance fluidized bed drying of Ascophyllum Nodosum: Drying kinetics and product quality assessment. *Ultrasonics Sonochemistry, 70*, Article 105298. https://doi.org/10.1016/j.ultsonch.2020.105298. July 2020.